Published in final edited form as:
Biochem J. 2013 January 1; 449(1): 167–173. doi:10.1042/BJ20121271.

Cytosolic [Ca^{2+}] regulation of $InsP_3$-evoked puffs

Michiko Yamasaki-Mann[1,*], **Angelo Demuro**[*], and **Ian Parker**[*,†]

[*]Department of Neurobiology and Behavior, University of California, Irvine, CA 92697

[†]Department of Physiology and Biophysics, University of California, Irvine, CA 92697

Synopsis

Inositol trisphosphate ($InsP_3$)-mediated puffs are fundamental building blocks of cellular Ca^{2+} signalling, and arise through the concerted opening of clustered $InsP_3$ receptors ($InsP_3Rs$) coordinated via Ca^{2+}-induced Ca^{2+} release. Although the Ca^{2+} dependency of $InsP_3Rs$ has been extensively studied at the single channel level, little is known as to how changes in basal cytosolic [Ca^{2+}] would alter dynamics of $InsP_3$-evoked Ca^{2+} signals in intact cells. To explore this question, we expressed Ca^{2+}-permeable channels (nicotinic acetylcholine receptors) in the plasma membrane of voltage-clamped *Xenopus* oocytes to regulate cytosolic [Ca^{2+}] by changing the electrochemical gradient for extracellular Ca^{2+} entry, and imaged Ca^{2+} liberation evoked by photolysis of caged $InsP_3$. Elevation of basal cytosolic [Ca^{2+}] strongly increased the amplitude and shortened the latency of global Ca^{2+} waves. In oocytes loaded with EGTA to localize Ca^{2+} signals, the number of sites at which puffs were observed, and the frequency and latency of puffs were strongly dependent on cytosolic [Ca^{2+}], whereas puff amplitudes were only weakly affected. Our result indicates that basal cytosolic [Ca^{2+}] strongly affects the triggering of puffs, but has less effect on puffs once they have been initiated.

Keywords

Ca^{2+} puffs; $InsP_3$; cytosolic Ca^{2+}; $InsP_3$ receptor

INTRODUCTION

The inositol 1, 4, 5 trisphosphate receptor ($InsP_3R$) is a Ca^{2+}-permeable channel expressed in the endoplasmic reticulum (ER) which is gated by the binding of the second messenger $InsP_3$ and by cytosolic Ca^{2+} itself [1–7]. Ca^{2+} liberation occurs at discrete functional release sites, formed by clusters of $InsP_3R$ on the endoplasmic reticulum (ER) membrane. These participate in generating a hierarchy of cellular Ca^{2+} signals involving opening of single $InsP_3R$ channels [8, 9], concerted release from several channels within a cluster [10], and global Ca^{2+} waves that propagate from cluster to cluster [11, 12]. The positive feedback mechanism of Ca^{2+}-induced Ca^{2+} release (CICR) by which Ca^{2+} released from one $InsP_3R$ channel promotes opening of neighbouring channels underlies these processes, and factors including cytosolic Ca^{2+} buffering, [$InsP_3$], and basal cytosolic [Ca^{2+}] determine the transition between local and global signalling patterns.

The role of cytosolic Ca^{2+} in modulating $InsP_3R$ channel gating has been extensively studied by single-channel recordings from $InsP_3R$ in excised nuclei and after reconstitution in lipid bilayers, revealing the well-known 'bell-shaped' curve of Ca^{2+} facilitation and

[1]Corresponding author: Michiko Yamasaki-Mann Department of Physiology, Anatomy and Genetics, University of Oxford, Le Gros Clark Building, South Parks Road, Oxford, U.K., Tel.: +44-1865 272178, Fax.: +44-1865 272420, michiko.yamasaki-mann@dpag.ox.ac.uk.

inhibition [1, 2, 13, 14]. However, less is known of how cytosolic Ca^{2+} modulates local $InsP_3$-mediated signals in the intact cell, although imaging studies in *Xenopus* oocytes demonstrate a profound potentiation of global Ca^{2+} waves [13, 15–17].

Here, we expressed Ca^{2+}-permeable nicotinic acetylcholine receptor/channels (nAChRs) in the plasma membrane of *Xenopus* oocytes so as to experimentally regulate basal cytosolic [Ca^{2+}] concentration [18], and examined how elevations of cytosolic [Ca^{2+}] affected the dynamics of local and global Ca^{2+} signals evoked by photoreleased $InsP_3$. We show that an increased probability of triggering local Ca^{2+} release at puff sites underlies the strong augmentation of global $InsP_3$-mediated Ca^{2+} waves, whereas puff amplitudes and durations were unaffected.

EXPERIMENTAL

Oocyte preparation and expression of nAChRs

Xenopus laevis were purchased from Nasco International (Fort Atkinson, WI, USA), and oocytes were surgically removed [19] following protocols approved by the UC Irvine Institutional Animal Care and Use committee. Stage V–VI oocytes were isolated and treated with collagenase (1 mg/ml of collagenase type A1 for 30 min) to remove follicular cell layers. One day after isolation oocytes were injected with a cRNA mixtures for nAChR expression (α,β,γ,δ subunits at a ratio of 2: 1: 1: 1; 50 nl at final concentration of 0.1–1 mg/ml) and were then maintained in modified Barth's solution (mM: NaCl, 88; KCl, 1; $NaHCO_3$, 2.4; $MgSO_4$, 0.82; $Ca(NO_3)_2$, 0.33; $CaCl_2$, 0.41; HEPES, 5; gentamicin, 1mg/ml ; pH 7.4) for 1 – 3 days at 16 °C before use. Expression of nAChR was evaluated using a voltage clamp to measure currents evoked by 500 nM ACh: oocytes showing currents >1 μA at −80 mV were selected for experiments.

Microinjection of oocytes

Intracellular microinjections were performed using a Drummond microinjector. About 1 h before Ca^{2+} imaging experiments, oocytes in Ca^{2+} -free Barth's solution were injected with Fluo–4 dextran (high affinity; K_d = 800 nM) to a final concentration of 40 μM, assuming equal distribution throughout a cytosolic volume of 1 μl, and with caged Ins (1,4,5) P_3 (D-myo-inositol 1,4,5-trisphosphate $P^{4(5)}$-[1-(2-nitrophenyl)ethyl]ester (final concentration 8 μM). EGTA (final concentration 300 μM) was further injected for puff studies.

Ca^{2+} imaging and flash photolysis

Oocytes were voltage-clamped using a conventional two-microelectrode technique. The membrane potential was held at 0 mV during superfusion with a non-desensitizing concentration of ACh (100 – 500 nM) in Ringer's solution and was briefly stepped to −120 mV to strongly increase the electrical driving force for Ca^{2+} influx [20]. Global Ca^{2+} signals were imaged at room temperature by a custom-build confocal line scanner [21] interfaced to an Olympus inverted microscope IX 70, and fluorescence excitation was provided by the 488 nm line of an argon ion laser, with the laser spot focused by a 40 × oil immersion objective (NA 1.35) and scanned along at a rate of 10 ms /50 μm line. To image puffs, we applied a wide-field fluorescence microscopy using an Olympus IX 71 inverted microscope equipped with a 40 × oil-immersion objective, a 488 nm argon ion laser for fluorescence excitation and an electron-multiplied charge-coupled device (ccd) camera (Cascade 128+: Roper Scientific) for imaging fluorescence emission (510–600 nm) at frame rates of 500 s^{-1}. Fluorescence was imaged from a 40 × 40 μm (128 × 128 pixel) region within the animal hemisphere of the oocyte. Fluorescence measurements made by line-scan and camera imaging are expressed as a ratio ($\Delta F/F_o$) of the mean change in fluorescence (ΔF) at a pixel relative to the resting fluorescence at that pixel before stimulation (F_o). Mean values of F_o

were obtained by averaging over several scans/frames before stimulation. To calibrate changes in $\Delta F/F_o$ values in terms of nM increases of free $[Ca^{2+}]$ we determined maximal (F_{max}) and minimal (F_{min}) fluorescence values by injecting Fluo-4 dextran-loaded oocytes (n = 5) with, respectively, 30 nl of 100 mM $CaCl_2$ or 100 mM EGTA from a micropipette located close to the imaging site. After correcting for oocyte autofluorescence, mean values were F_{max} = 8.52 ± 1.16, F_{min} = 0.857 ± 0.024 relative to a resting fluorescence F_0 before injection. We assumed a K_d for fluo-4 dextran of 2400nM, based on measurements of ~800 nM in free solution [22] and a roughly three-fold reduction in affinity in cytoplasmic environment [22]. A fluorescence increase of $\Delta F/F_o$ = 1 above baseline would then correspond to an increase of $[Ca^{2+}]_{cyt}$ of about 360 nM. Photolysis of caged IP_3 was evoked by flashes of UV light (350–400 nm) from a mercury arc lamp, delivered through the microscope objective and adjusted to uniformly irradiate a circular region slightly larger than the imaging frame or scan line. Flash durations were set using a Uniblitz shutter and digital controller.

Reagents

Fluo-4 dextran, high affinity (K_d: ~800nM), and caged $InsP_3$ were purchased from Invitrogen (Carlsbad, CA, U.S.A.). All other reagents were from Sigma-Aldrich (St. Louis, MO, U.S.A.).

Data analysis

Custom routines written in the IDL programming environment (Research Systems, Boulder, CO, USA) were used for line scan image processing and measurements. MetaMorph (Molecular Devices) was used to process and measure data obtained from wide-field camera-based imaging. Further analysis and graphing was accomplished using Microcal Origin version 6.0 (OriginLab, Northamptom, MA, USA). Data are expressed as mean ± 1 SEM, and significance was assessed by t-tests.

RESULTS

Elevated basal cytosolic $[Ca^{2+}]$ enhances $InsP_3$-evoked Ca^{2+} waves

In order to evoke cytosolic $[Ca^{2+}]$ elevations, Ca^{2+} influx was induced through nAChRs expressed in the oocyte plasma membrane. Oocytes were continuously superfused with Ringer's solution containing 1.8 mM Ca^{2+} together with a low, non-desensitizing concentration (100 – 500 nM) of acetylcholine, and were voltage-clamped to control the electrochemical gradient for Ca^{2+} entry. The membrane potential was held at 0 mV to minimize Ca^{2+} influx, and was then stepped to more negative values to promote Ca^{2+} influx, beginning 2.5 s before delivery of a UV flash to photorelease $InsP_3$ from a caged precursor loaded into the oocyte (Fig. 1A). The resulting changes in Fluo-4 fluorescence were imaged to compare $InsP_3$-evoked Ca^{2+} responses evoked by identical UV flashes during cytosolic $[Ca^{2+}]$ elevation with control records when the voltage pulse was not applied.

We first examined global Ca^{2+} signals evoked in oocytes that were not loaded with EGTA. The panels on the left of Figure 1B show representative linescan images of fluorescence changes evoked by photoreleased $InsP_3$ without (top) and with (bottom) Ca^{2+} influx; corresponding florescence profiles are presented on the right. We compared the latencies and peak amplitude of $InsP_3$-evoked Ca^{2+} signals under resting cytosolic $[Ca^{2+}]$, and during Ca^{2+} influx that increased the basal fluorescence signal by a mean of 0.60 ± 0.06 $\Delta F/F_o$ (6 oocytes from 3 different frogs). Latencies (time from the UV flash to the initial rise of fluorescence) were significantly shorter during cytosolic $[Ca^{2+}]$ elevation (Fig. 1C: control, 284 ± 14 ms: during Ca^{2+} influx, 177 ± 30 ms, $p < 0.05$). The mean peak amplitude of Ca^{2+} waves was profoundly augmented by cytosolic Ca^{2+} elevation (Fig. 1D: control, $\Delta F/Fo$ =

1.68 ± 0.23; during Ca^{2+} influx; ΔF/Fo = 3.50 0.45, p < 0.05, n = 6). These results are consistent with previous observations showing facilitation of $InsP_3$-evoked Ca^{2+} signals by cytosolic [Ca^{2+}] [1–6] [7].

Elevated basal cytosolic [Ca^{2+}] promotes $InsP_3$-evoked Ca^{2+} puffs

We next examined the effects of basal cytosolic [Ca^{2+}] elevations on local Ca^{2+} puffs. For this purpose oocytes were loaded with EGTA (final intracellular concentration 300 μM) to suppress generation of Ca^{2+} waves by inhibiting inter-cluster diffusion of Ca^{2+} ions [23]. We further employed wide-field fluorescence microscopy to image a 40 × 40 μm field of view with a fast (500 fps) electron-multiplied c.c.d. camera, so as to sample many more puff sites than possible by one-dimensional linescan imaging. Figure 2 shows the experimental protocol (Fig. 2Aa), and representative fluorescence traces monitored from small regions of interest centred on puff sites illustrating responses evoked by photoreleased $InsP_3$ at resting cytosolic Ca^{2+} (Fig. 2Ab) and when Ca^{2+} was elevated by Ca^{2+} influx (Fig. 2Ac,d). The photolysis flash was delivered 4 s after the onset of the hyperpolarizing pulse so as to allow cytosolic [Ca^{2+}] to equilibrate, and puffs were then recorded for 6 s while the hyperpolarization was maintained. We varied the duration of the photolysis flash to evoke differing numbers of puffs at resting cytosolic [Ca^{2+}]; 'weak' flashes (25 – 50 ms) were chosen to evoke on average about a single puff in the entire imaging field 40 × 40 μm, and 'strong' flashes (50 – 100 ms) to evoke up to 4 puffs. Even the 'strong' stimulus was chosen to evoke responses well below the maximal, so as to avoid possible saturation effects when responses were further potentiated by Ca^{2+} influx.

Figure 2B shows a scatter plot of the relationship between the numbers of individual sites in the imaging field where puffs were observed during 6 s following photorelease of $InsP_3$ as a function of the elevation of cytosolic [Ca^{2+}] evoked by hyperpolarizing pulses. We express the [Ca^{2+}] elevation in terms of fluorescence ratio change, without correction for oocyte autofluorescence (about 50% of resting Fluo-4 fluorescence). Based on the calibration described in Methods, an increase of $\Delta F/F_o$ of 0.1 corresponds to a rise in [Ca^{2+}] of about 36 nM. With both weak and strong photolysis flashes the numbers of responding puff sites increased steeply with increasing basal cytosolic [Ca^{2+}], with strong flashes giving greater numbers at any given basal [Ca^{2+}]. Fig. 2C shows mean data, grouped according to flash duration and whether basal cytosolic levels just before the photolysis flash were at or close to the resting level ($\Delta F/F_o$ 0 – 0.1) or were appreciably elevated (ΔF/Fo > 0.1).

Elevated cytosolic [Ca^{2+}] shortens puff latency

Figures 3A and B show scatter plots of individual and mean latencies of puffs, grouped according to cytosolic [Ca^{2+}] elevation at the time of the photolysis flash. Puffs evoked by weak stimuli arose with relatively long (2–3s) latencies, which tended to shorten with increasing cytosolic [Ca^{2+}] but did not show a statistically significant correlation (Fig. 3A). On the other hand, mean puff latencies were shorter with stronger photorelease of $InsP_3$ (Fig. 3B), and showed a marked dependence on cytosolic [Ca^{2+}], reducing from 2133 ± 200 ms at near resting level (ΔF/F <0.1) to 1240 ± 174 ms when the fluorescence was elevated to >0.1 $\Delta F/F_o$ during Ca^{2+} influx ($p < 0.01$). Puff latencies followed roughly exponential distributions at both relatively low and high cytosolic [Ca^{2+}] (Figs. 3C and D, respectively), with a markedly shorter time constant at higher [Ca^{2+}] (Fig. 3C and D).

Puff amplitude are only weakly dependent on cytosolic [Ca^{2+}]

Next, we analyzed the effects of changes in cytosolic [Ca^{2+}] on puff amplitudes. After pooling data across all different basal cytosolic [Ca^{2+}] levels we found no significant difference in mean puff amplitudes evoked by weak or strong photorelease of $InsP_3$ (Fig. 4A, weak flash mean puff amplitude ΔF/Fo = 0.43 ± 0.04, n = 56; strong flash, ΔF/Fo =

0.42 ± 0.03, n = 155, p > 0.05). Looking then at the effect of elevating cytosolic [Ca^{2+}] levels, we observed little or no effect on the amplitudes of puffs evoked by weak photorelease (Fig. 4B). On the other hand, puffs evoked by strong photorelease of $InsP_3$ showed a significant increase in puff amplitude with higher elevations of cytosolic [Ca^{2+}] ($\Delta F/Fo > 0.2$) (Fig. 4C).

Puff durations are independent of basal cytosolic [Ca^{2+}]

We had previously observed a prolongation of puff duration when puffs were evoked after loading ER Ca^{2+} stores by inducing a prior Ca^{2+} influx in oocytes transfected to over-express SERCA, but not in control (non-expressing) oocytes. We now examined the effect of elevated $[Ca^{2+}]_{cyt}$ on puff durations. Puffs evoked by strong photorelease of $InsP_3$ were compared in the same imaging field at basal $[Ca^{2+}]_{cyt}$ and during induction of Ca^{2+} influx. Figure 5A shows a scatter plot of durations of puffs (measured as full duration at half-maximal amplitude: FDHM) against the latency of the puffs following the UV flash. No differences were apparent in puff durations between control and Ca^{2+} influx records, and puff durations did not show any obvious systematic dependence on latency following the UV flash. Figure 5B further plots mean values of FDHM of control puffs and puffs during Ca^{2+} influx, showing no significant difference. [$p = 0.64$].

DISCUSSION

The aim of the present study was to investigate how elevated basal cytosolic [Ca^{2+}] would affect $InsP_3$-evoked Ca^{2+} signals. We utilized the expression of Ca^{2+}-permeable nicotinic receptor/channels in the plasma membrane as a means to evoke controlled entry of extracellular Ca^{2+} into the cell during hyperpolarizing voltage-clamped pulses. Consistent with previous observations [4, 5], we confirmed that cytosolic [Ca^{2+}] elevations powerfully facilitated $InsP_3$-mediated Ca^{2+} waves in terms of increased peak amplitude and shortened latency (Figures 1A and B). We further investigated the effect of elevated basal $[Ca^{2+}]_{cyt}$ on the local $InsP_3$-mediated Ca^{2+} puffs that are the triggers and fundamental building blocks of Ca^{2+} waves, as well as serving signalling functions in their own right. Our results show that the numbers of puff sites that respond at a given [$InsP_3$] are strongly potentiated in a graded manner with increasing $[Ca^{2+}]_{cyt}$, and that the mean latency of puffs markedly shortens. In contrast, puff amplitudes were little affected except at high $[Ca^{2+}]_{cyt}$, and we observed no significant effects of $[Ca^{2+}]_{cyt}$ on puff durations.

The effects we describe on $InsP_3$-evoked Ca^{2+} liberation from the ER can be directly attributed to changes in basal $[Ca^{2+}]_{cyt}$, and not to any increase in Ca^{2+} store filling within the ER. We had previously utilized Ca^{2+} influx through nicotinic receptors as a means to increase ER Ca^{2+} loading, by applying a transient hyperpolarizing pulse and then allowing $[Ca^{2+}]_{cyt}$ to subside to the resting level before examining responses to photoreleased $InsP_3$. However, changes in puff properties were observed only when SERCA activity was accelerated by cADP ribose [20] [24] or when SERCA 2b was overexpressed [18]. With basal SERCA activity, no significant changes in puff triggering, kinetics or amplitude were apparent following even strong Ca^{2+} influx.

We have proposed that the puff is itself triggered by the stochastic opening of a single $InsP_3R$ channel within the cluster [25, 26]. Factors that determine the occurrence of puffs thus include the number of channels present in the cluster and the open probability of each channel. The latter, in turn, is a function of the concentrations of $InsP_3$ and Ca^{2+}, acting as co-agonists to open the channel [3, 7, 27]. Concordant with this mechanism, increasing [$InsP_3$] results in an increased frequency of puffs and a shortening of the latency to the first puff evoked at a site following photorelease of $InsP_3$ [26, 28]). Similarly, modest elevations of $[Ca^{2+}]_{cyt}$ will increase the open channel probability at a given [$InsP_3$], and hence increase

the probability of puff triggering, leading to a greater number of sites that generate puffs following photorelease of $InsP_3$ and a shortening in mean latency of these puffs. Although gating of the $InsP_3R$ channel is biphasically regulated by $[Ca^{2+}]$, inhibition of the native *Xenopus* $InsP_3R$ arises only when $[Ca^{2+}]$ exceeds several hundred μM [27] and thus would not be expected to be apparent in our experiments, where we estimate that the maximal Ca^{2+} influx ($\Delta F/F_o \sim 0.3$) corresponded to an increase of $[Ca^{2+}]_{cyt}$ of < 100 nM.

Because the resting $[Ca^{2+}]_{cyt}$ is very low, small elevations above this level will strongly potentiate puff triggering. On the other hand, once an initial 'trigger' channel opens, the Ca^{2+} flux passing through it will elevate the local free $[Ca^{2+}]$ at the puff site to much higher levels, predicted to reach a few hundred μM at the mouth of the open channel and at least several μM at neighboring $InsP_3R$ within the cluster [29]. This will effectively 'swamp' the effect of any smaller elevation of basal $[Ca^{2+}]$. Once triggered, the puff thus becomes a self-regenerative process and its subsequent evolution is expected to be substantially independent of the preceding conditions; likely explaining why we found little dependence of puff amplitudes and kinetics on basal $[Ca^{2+}]_{cyt}$.

The sensitization of global Ca^{2+} waves by elevated basal $[Ca^{2+}]_{cyt}$ may similarly be explained by enhanced coupling between neighbouring release sites. Ca^{2+} waves propagate because Ca^{2+} released from one site diffuses to evoke CICR from adjacent sites [11, 12], and this triggering will be facilitated if $[Ca^{2+}]_{cyt}$ is already elevated. The results in Fig. 1 were obtained using relatively weak photorelease of $InsP_3$ that evoked only abortive Ca^{2+} waves, and basal $[Ca^{2+}]$ elevation promoted a more robust propagation by CICR resulting in strong potentiation of the spatially-averaged Ca^{2+} signal. With stronger stimulation by $InsP_3$ the amplitude of repetitive Ca^{2+} waves is not potentiated by Ca^{2+} influx [17], presumably because the more substantial Ca^{2+} release through $InsP_3R$ swamps any effect of elevated basal $[Ca^{2+}]$, but wave velocities and frequency of repetitive spikes are increased [17].

$InsP_3$-mediated Ca^{2+} signalling can function as a coincidence detector, whereby release of Ca^{2+} from intracellular stores is potentiated by extracellular Ca^{2+} entering through plasmalemmal ligand- or voltage-operated channels. This interaction may arise through two different mechanisms, operating on different timescales. Most directly, as we describe here, elevation of basal $[Ca^{2+}]_{cyt}$ enhances the probability of triggering of local and global $[Ca^{2+}]$ signals by binding to activating sites on the cytosolic face of the $InsP_3R$. In addition, we have described a more circuitous mechanism, whereby extracellular $[Ca^{2+}]$ entering the cytosol is taken up by the action of SERCA pumps, leading to enhanced filling of ER Ca^{2+} stores [18]. That, in turn, promotes Ca^{2+} puffs and waves, likely because increased Ca^{2+} flux through the $InsP_3R$ channel enhances CICR via the cytosolic activating sites on the $InsP_3R$, and possibly also through luminal regulation of $InsP_3R$ function [30–32]. The direct action of Ca^{2+} influx on $InsP_3R$ is immediate and short lasting, depending on clearance rate from the cytosol. In contrast, potentiation via ER store filling is slower to develop, more persistent, and subject to potential modulation by other messenger pathways, such as cADPR, that affect SERCA activity either directly or indirectly [20, 33, 34]. Interactions between these different modulatory mechanisms are likely to be of particular importance for Ca^{2+} signalling in neurons in regard to activity-dependent synaptic plasticity as well as gene expression and protein synthesis [35–37].

Acknowledgments

FUNDING

This work was supported by a grant (GM048071) from the National Institutes of Health.

Abbreviations used

InsP3	Inositol trisphosphate
caged InsP3	Ins (1,4,5) P_3 (D-myo-inositol 1,4,5-trisphosphate $P^{4(5)}$-[1-(2-nitrophenyl)ethyl]ester
CICR	Ca^{2+}-induced Ca^{2+} release
nAChRs	nicotinic acetylcholine receptor/channels
ER	the endoplasmic reticulum
SERCA	the sarcoplasmic/endoplasmic reticulum calcium ATPase

REFERENCES

1. Iino M. Biphasic Ca2+ dependence of inositol 1,4,5-trisphosphate-induced Ca release in smooth muscle cells of the guinea pig taenia caeci. J. Gen. Physiol. 1990; 95:1103–1122. [PubMed: 2373998]
2. Bezprozvanny I, Watras J, Ehrlich BE. Bell-shaped calcium-response curves of Ins(1,4,5)P3- and calcium-gated channels from endoplasmic reticulum of cerebellum. Nature. 1991; 351:751–754. [PubMed: 1648178]
3. Finch EA, Turner TJ, Goldin SM. Calcium as a coagonist of inositol 1,4,5-trisphosphate-induced calcium release. Science. 1991; 252:443–446. [PubMed: 2017683]
4. Yao Y, Parker I. Potentiation of inositol trisphosphate-induced Ca2+ mobilization in Xenopus oocytes by cytosolic Ca2+ J. Physiol. 1992; 458:319–338. [PubMed: 1284567]
5. DeLisle S, Welsh MJ. Inositol trisphosphate is required for the propagation of calcium waves in Xenopus oocytes. J. Biol. Chem. 1992; 267:7963–7966. [PubMed: 1569053]
6. Marshall IC, Taylor CW. Biphasic effects of cytosolic Ca2+ on Ins(1,4,5)P3-stimulated Ca2+ mobilization in hepatocytes. J. Biol. Chem. 1993; 268:13214–13220. [PubMed: 8514760]
7. Marchant JS, Taylor CW. Cooperative activation of IP3 receptors by sequential binding of IP3 and Ca2+ safeguards against spontaneous activity. Curr. Biol. 1997; 7:510–518. [PubMed: 9210378]
8. Parker I, Choi J, Yao Y. Elementary events of InsP3-induced Ca2+ liberation in Xenopus oocytes: hot spots, puffs and blips. Cell calcium. 1996; 20:105–121. [PubMed: 8889202]
9. Parker I, Yao Y. Ca2+ transients associated with openings of inositol trisphosphate-gated channels in Xenopus oocytes. J. Physiol. 1996; 491(Pt 3):663–668. [PubMed: 8815201]
10. Parker I, Yao Y. Regenerative release of calcium from functionally discrete subcellular stores by inositol trisphosphate. Proc. Biol. Sci. 1991; 246:269–274. [PubMed: 1686093]
11. Marchant JS, Parker I. Role of elementary Ca(2+) puffs in generating repetitive Ca(2+) oscillations. EMBO J. 2001; 20:65–76. [PubMed: 11226156]
12. Dawson SP, Keizer J, Pearson JE. Fire-diffuse-fire model of dynamics of intracellular calcium waves. Proc. Natl. Acad. Sci. U S A. 1999; 96:6060–6063. [PubMed: 10339541]
13. Parker I, Ivorra I. Inhibition by Ca2+ of inositol trisphosphate-mediated Ca2+ liberation: a possible mechanism for oscillatory release of Ca2+ Proc. Natl. Acad. Sci. U S A. 1990; 87:260–264. [PubMed: 2296584]
14. Mak DO, Pearson JE, Loong KP, Datta S, Fernandez-Mongil M, Foskett JK. Rapid ligand-regulated gating kinetics of single inositol 1,4,5-trisphosphate receptor Ca2+ release channels. EMBO Rep. 2007; 8:1044–1051. [PubMed: 17932510]
15. Lechleiter JD, Clapham DE. Molecular mechanisms of intracellular calcium excitability in X. laevis oocytes. Cell. 1992; 69:283–294. [PubMed: 1568248]
16. Meyer T. Cell signaling by second messenger waves. Cell. 1991; 64:675–678. [PubMed: 1997202]
17. Yao Y, Parker I. Ca2+ influx modulation of temporal and spatial patterns of inositol trisphosphate-mediated Ca2+ liberation in Xenopus oocytes. J. Physiol. 1994; 476:17–28. [PubMed: 8046631]
18. Yamasaki-Mann M, Parker I. Enhanced ER Ca2+ store filling by overexpression of SERCA2b promotes IP3-evoked puffs. Cell calcium. 2011; 50:36–41. [PubMed: 21616533]

19. Demuro A, Parker I. "Optical patch-clamping": single-channel recording by imaging Ca2+ flux through individual muscle acetylcholine receptor channels. The Journal of general physiology. 2005; 126:179–192. [PubMed: 16103278]
20. Yamasaki-Mann M, Demuro A, Parker I. cADPR stimulates SERCA activity in Xenopus oocytes. Cell calcium. 2009; 45:293–299. [PubMed: 19131109]
21. Parker I, Callamaras N, Wier WG. A high-resolution, confocal laser-scanning microscope and flash photolysis system for physiological studies. Cell calcium. 1997; 21:441–452. [PubMed: 9223680]
22. Martin VV, Beierlein M, Morgan JL, Rothe A, Gee KR. Novel fluo-4 analogs for fluorescent calcium measurements. Cell calcium. 2004; 36:509–514. [PubMed: 15488600]
23. Dargan SL, Parker I. Buffer kinetics shape the spatiotemporal patterns of IP3-evoked Ca2+ signals. J. Physiol. 2003; 553:775–788. [PubMed: 14555715]
24. Yamasaki-Mann M, Demuro A, Parker I. Modulation of Endoplasmic Reticulum Ca(2+) Store Filling by Cyclic ADP-ribose Promotes Inositol Trisphosphate (IP(3))-evoked Ca(2+) Signals. J. Biol. Chem. 2010; 285:25053–25061. [PubMed: 20538594]
25. Rose HJ, Dargan S, Shuai J, Parker I. 'Trigger' events precede calcium puffs in Xenopus oocytes. Biophys J. 2006; 91:4024–4032. [PubMed: 16980363]
26. Dickinson GD, Swaminathan D, Parker I. The probability of triggering calcium puffs is linearly related to the number of inositol trisphosphate receptors in a cluster. Biophysical journal. 2012; 102:1826–1836. [PubMed: 22768938]
27. Foskett JK, White C, Cheung KH, Mak DO. Inositol trisphosphate receptor Ca2+ release channels. Physiol. Rev. 2007; 87:593–658. [PubMed: 17429043]
28. Shuai J, Pearson JE, Foskett JK, Mak DO, Parker I. A kinetic model of single and clustered IP3 receptors in the absence of Ca2+ feedback. Biophysical journal. 2007; 93:1151–1162. [PubMed: 17526578]
29. Ullah G, Parker I, Mak DO, Pearson JE. Multi-scale data-driven modeling and observation of calcium puffs. Cell calcium. 2012
30. Horne JH, Meyer T. Luminal calcium regulates the inositol trisphosphate receptor of rat basophilic leukemia cells at a cytosolic site. Biochemistry. 1995; 34:12738–12746. [PubMed: 7548027]
31. Sienaert I, De Smedt H, Parys JB, Missiaen L, Vanlingen S, Sipma H, Casteels R. Characterization of a cytosolic and a luminal Ca2+ binding site in the type I inositol 1,4,5-trisphosphate receptor. J. Biol. Chem. 1996; 271:27005–27012. [PubMed: 8900188]
32. Higo T, Hattori M, Nakamura T, Natsume T, Michikawa T, Mikoshiba K. Subtype-specific and ER lumenal environment-dependent regulation of inositol 1,4,5-trisphosphate receptor type 1 by ERp44. Cell. 2005; 120:85–98. [PubMed: 15652484]
33. Lukyanenko V, Gyorke I, Wiesner TF, Gyorke S. Potentiation of Ca(2+) release by cADP-ribose in the heart is mediated by enhanced SR Ca(2+) uptake into the sarcoplasmic reticulum. Circ. Res. 2001; 89:614–622. [PubMed: 11577027]
34. Macgregor AT, Rakovic S, Galione A, Terrar DA. Dual effects of cyclic ADP-ribose on sarcoplasmic reticulum Ca2+ release and storage in cardiac myocytes isolated from guinea-pig and rat ventricle. Cell calcium. 2007; 41:537–546. [PubMed: 17156839]
35. Rose CR, Konnerth A. Stores not just for storage. intracellular calcium release and synaptic plasticity. Neuron. 2001; 31:519–522. [PubMed: 11545711]
36. Barbara JG. IP3-dependent calcium-induced calcium release mediates bidirectional calcium waves in neurones: functional implications for synaptic plasticity. Biochimica et biophysica acta. 2002; 1600:12–18. [PubMed: 12445454]
37. Watanabe S, Hong M, Lasser-Ross N, Ross WN. Modulation of calcium wave propagation in the dendrites and to the soma of rat hippocampal pyramidal neurons. The Journal of physiology. 2006; 575:455–468. [PubMed: 16809362]

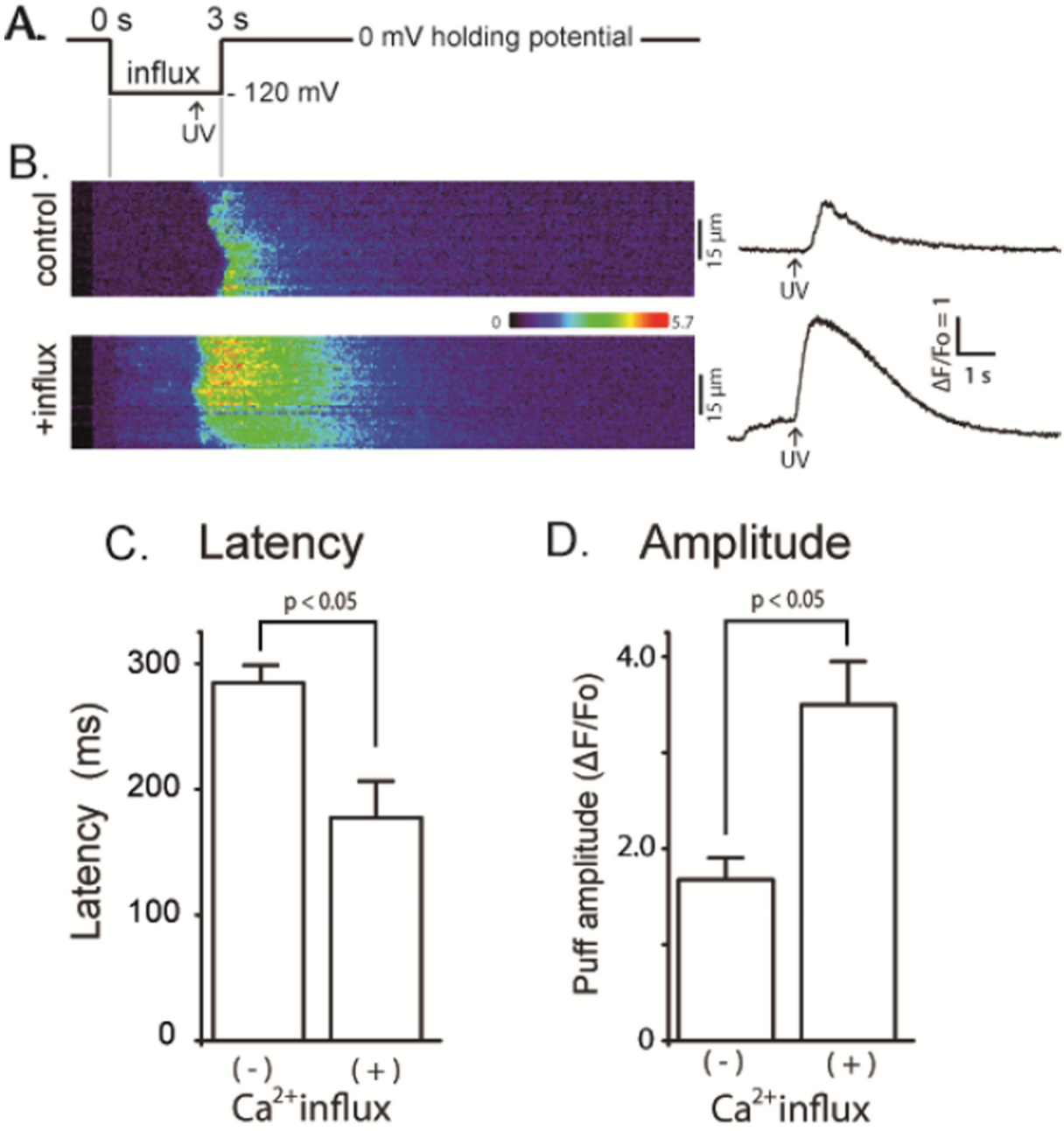

FIGURE 1. Elevated basal cytosolic [Ca^{2+}] enhances $InsP_3$-induced Ca^{2+} waves

(A) Schematic of the experimental protocol. **(B)** Representative confocal linescan images illustrating fluo-4 dextran fluorescence signals evoked by photoreleased $InsP_3$ under control conditions without elevation of cytosolic [Ca^{2+}] (upper) and with cytosolic [Ca^{2+}] elevation (lower). Increasing fluorescence ($\Delta F/F_o$: Ca^{2+} level) is depicted on a pseudocolor scale as indicated by the colour bar. Traces on the right show corresponding fluorescence profiles averaged across 15 µm widths of the linescans (indicated by bars). **(C)** Mean values of latency between the photolysis flash and initial rise in fluorescence derived from traces like those in (B). Latency without Ca^{2+} influx 284 ± 14 ms; during Ca^{2+} influx 177 ± 30 ms, p <

0.05. **(D)** Mean peak amplitudes of Ca^{2+} waves derived from traces like those in (B). $\Delta F/F_o$ without Ca^{2+} influx 1.68 ± 0.23; during Ca^{2+} influx 3.50 ± 0.45, $p < 0.05$: n = 6 and 4 oocytes, respectively).

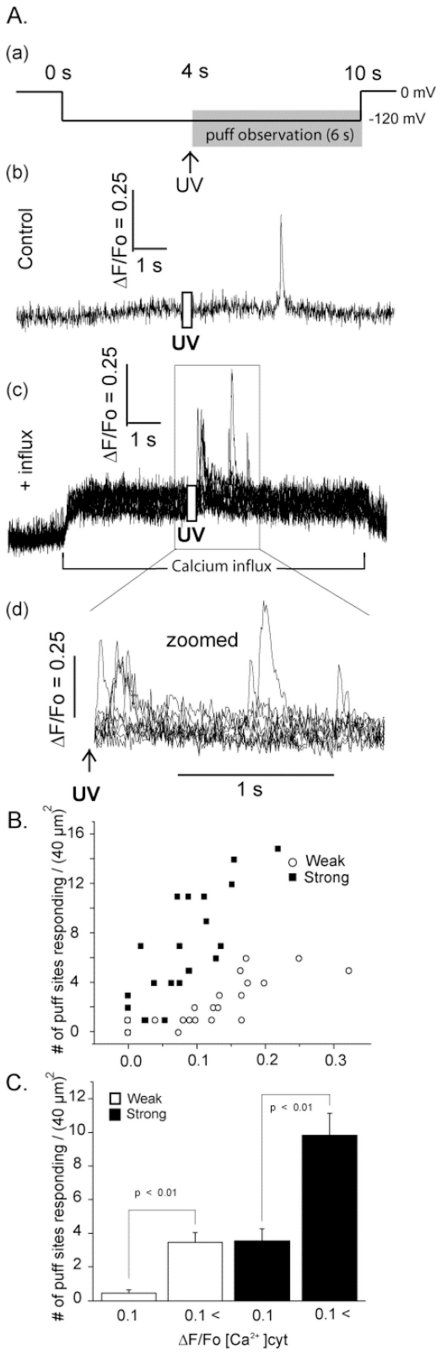

FIGURE 2. Cytosolic [Ca^{2+}]-dependent potentiation of $InsP_3$-evoked Ca^{2+} puffs

(A) (**a**) schematic of the experimental protocol. (**b,c**) Representative fluorescence profiles of puffs evoked, respectively, without (control) and with (+ influx) basal cytosolic [Ca^{2+}] elevation, obtained from the same oocyte. The record in (b) was obtained from the single responding site within the image field. That in (c) shows superimposed traces from 7 responding sites. (**d**) Zoomed version of (c) on an expanded timescale to illustrate more clearly the variation in puff latencies following photorelease of $InsP_3$. Traces in (b–d) are blanked out during the photolysis flash. **(B)** Scatter plot showing the numbers of sites within the imaging field that showed puffs following weak (open symbols; 25–50 ms flash duration) or strong (filled symbols; 50–100 ms) photorelease of $InsP_3$ as a function of

cytosolic Ca^{2+} elevation during influx ($\Delta F/Fo[Ca^{2+}]_{cyt}$). **(C)** Mean numbers of responding puff sites within imaging field, grouped by photolysis strength (weak, open bars; strong, filed bars) and by elevation of basal cytosolic $[Ca^{2+}]$ ($\Delta F/F_o < 0.1$ or > 0.1).

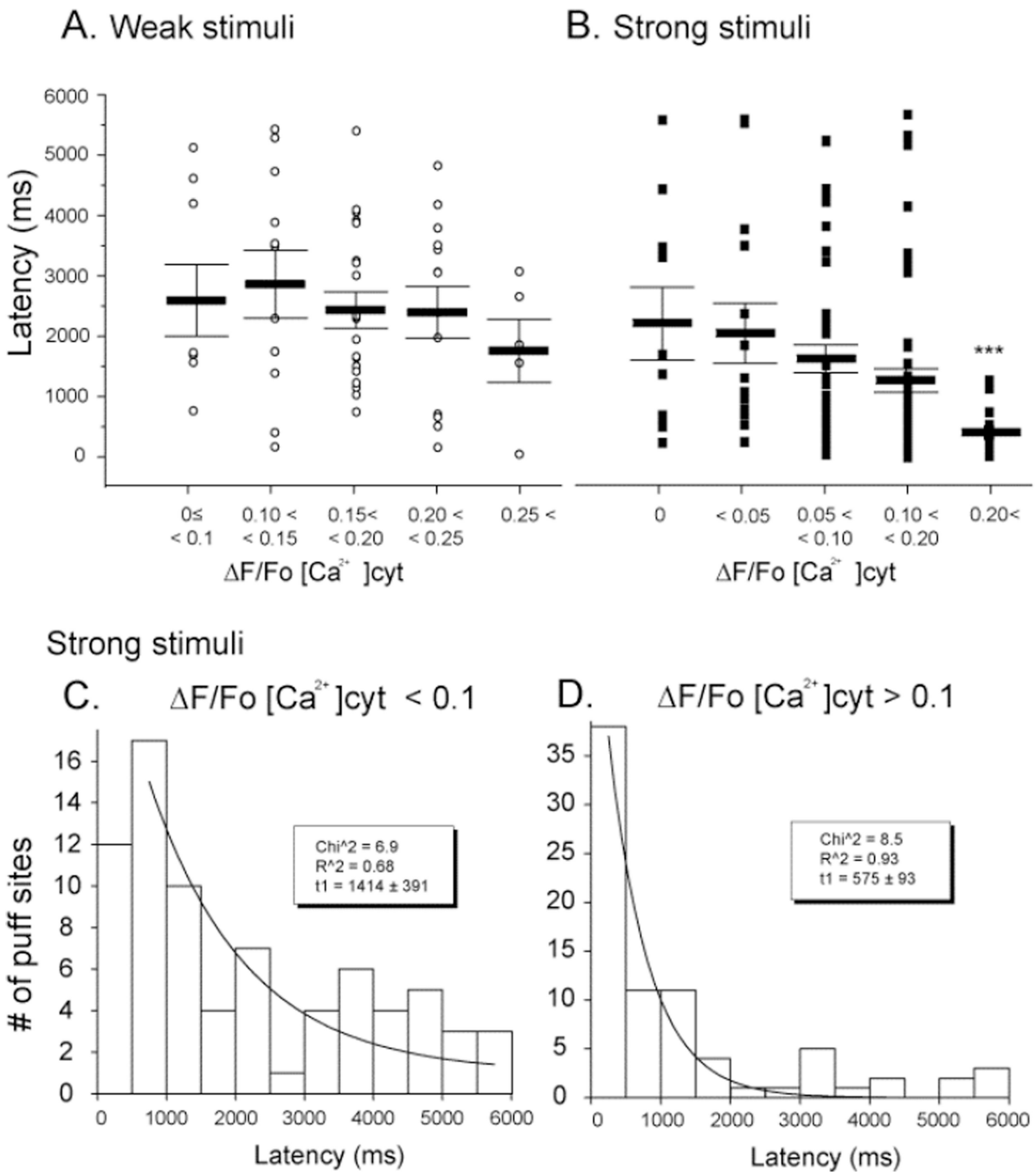

FIGURE 3. Puff latencies shorten with increasing cytosolic [Ca^{2+}]

Latencies were measured as the time from end of the photolysis flash to the observation of the first puff at a given site. (**A, B**) Mean latencies of puffs evoked, respectively, by weak and strong photorelease of $InsP_3$. Open circles in (A) and filled squares in (B) indicate data from individual puffs; bars indicate mean ± SEM. **(C, D)** Histograms showing distributions of latencies of puffs evoked by strong stimuli during cytosolic Ca^{2+} elevations < 0.1 $\Delta F/F_0$ (**C**) and > 0.1 (**D**) Curves are single exponential fits to the data with respective time constants of 1414 ± 391 ms and 575 ± 93 ms.

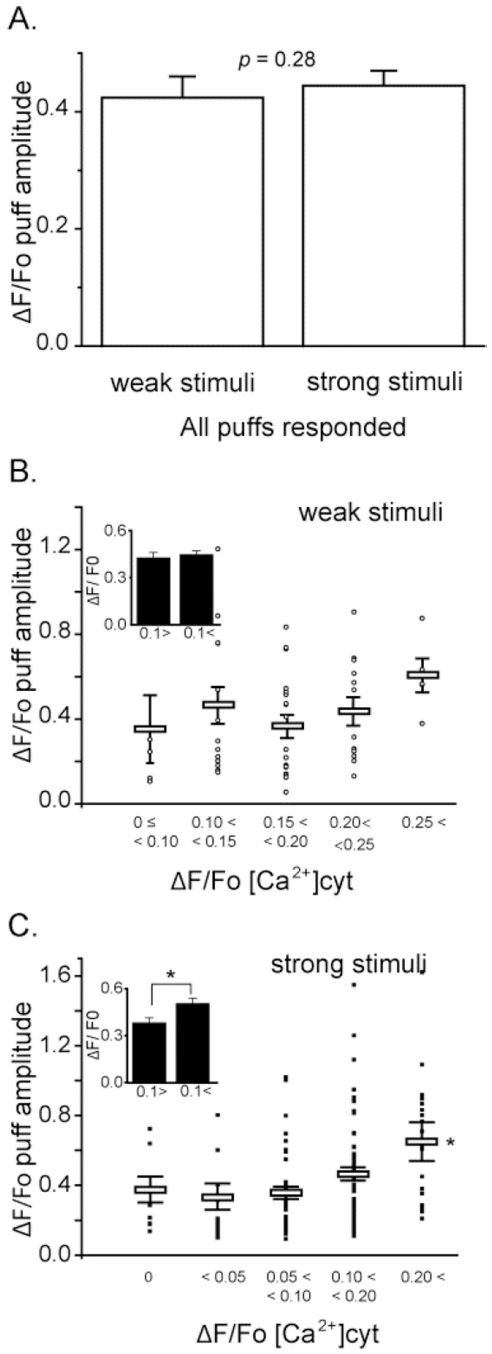

FIGURE 4. The amplitude of $InsP_3$-evoked puffs is only weakly dependent on the basal cytosolic $[Ca^{2+}]$

(A) Mean puff amplitudes evoked by weak photorelease of $InsP_3$ ($\Delta F/F_o$ = 0.42 ± 0.04, n = 56) and strong photorelease (ΔF/Fo = 0.44 ± 0.23, n = 146. $p > 0.05$), after pooling data across all basal cytosolic $[Ca^{2+}]$ levels. **(B)** Main panel shows a scatter plot of amplitudes ($\Delta F/F_0$) of puffs evoked by weak photorelease of $InsP_3$ as a function of increase in basal fluorescence during Ca^{2+} influx. Open circles mark data from individual puffs and bars show mean ± SEM. **(C)** Corresponding measurements of puff amplitudes following strong photorelease of $InsP_3$. Inset graphs in (B) and (C) represent mean values of puff amplitudes

evoked, respectively, by weak and strong photolysis flashes grouped for cytosolic [Ca^{2+}] elevations < 0.1 and > 0.1 $\Delta F/F_o$.

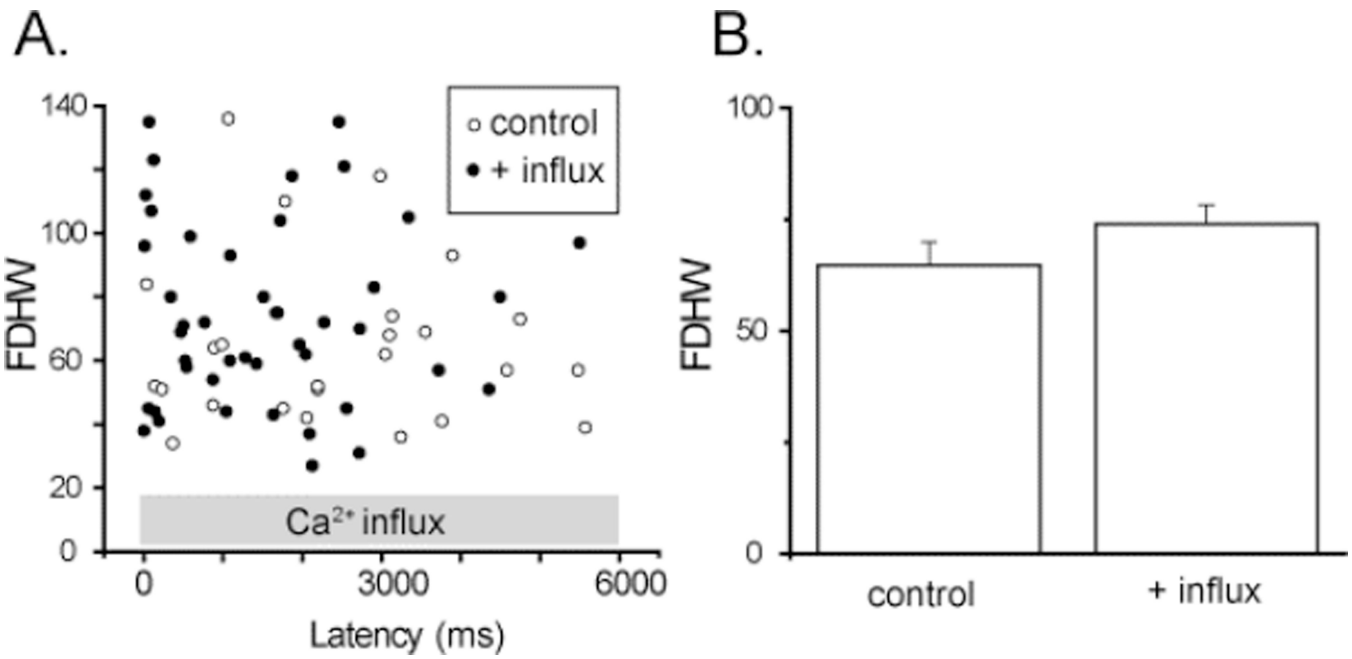

FIGURE 5. Duration of $InsP_3$-evoked puffs is independent on the basal cytosolic $[Ca^{2+}]$

(A) Scatter plot showing full-duration at half-maximal amplitude (FDHM) of all puffs observed within the imaging field as a function of their latencies. Open circles are control puffs evoked by the strong photolysis flash, and filled circles represents FDHM of puffs observed during Ca^{2+} influx (mean $\Delta F/Fo[Ca^{2+}]_{cyt}$ = 0.23 ± 0.03, 4 trials). **(B)** Mean FDHM of puffs. (control FDHM; 64.8 ± 5.2, n = 25, with influx; FDHM 64.8 ± 5.2, n = 44, 4 oocytes).